

# TR Invariant T.I.

Taper

April 27, 2017

## Abstract

An incomplete note of dissertation by Taylor Hughes [Hug09].

## Contents

<b>1</b>	<b>Spectrum of (2 + 1)d Lattice Dirac Model</b>	<b>1</b>
1.1	Numerical Solution in Infinity Cylinder Geometry . . . . .	2
1.1.1	Calculation Note I (Not related to the main discussion) . . . . .	5
1.2	Why I Think the Lattice Model Hamiltonian is Mildly Wrong	8
1.3	Solution With Translational Invariance (Bloch States) in both x and y (Infinite Plane) . . . . .	9
1.3.1	Numerical Solution . . . . .	9
1.4	Solution With Translational Invariance in x, and Open Boundary in y (Infinite Stripe) . . . . .	13
1.4.1	Edge States in Continuum Limit . . . . .	13
1.4.2	Edge State in Infinity Strip . . . . .	19
1.5	Berry Phase . . . . .	19
<b>2</b>	<b>License</b>	<b>22</b>
Start with chapter 2.		

## 1 Spectrum of (2+1)d Lattice Dirac Model

sec:2+1d-LDirac Model

$$H_{LD} = \sum_{m,n} \left\{ i \left[ c_{m+1,n}^\dagger \sigma^x c_{m,n} - c_{m,n}^\dagger \sigma^x c_{m+1,n} \right] + i \left[ c_{m,n+1}^\dagger \sigma^y c_{m,n} - c_{m,n}^\dagger \sigma^y c_{m,n+1} \right] \right. \\ \left. - \left[ c_{m+1,n}^\dagger \sigma^z c_{m,n} + c_{m,n}^\dagger \sigma^z c_{m+1,n} + c_{m,n+1}^\dagger \sigma^z c_{m,n} + c_{m,n}^\dagger \sigma^z c_{m,n+1} \right] \right. \\ \left. + (2-m)c_{m,n}^\dagger \sigma^z c_{m,n} \frac{\hbar}{2} \right\} \quad (1.0.1)$$

Above is the lattice model (eq.2.19) of [Hug09]. Here it should be noted that  $c_{m,n} = (c_{u,m,n}, c_{v,m,n})$  for two degrees of freedom.

## 1.1 Numerical Solution in Infinity Cylinder Geometry

This Hamiltonian is solved here with a infinite cylinder geometry, i.e. the lattice is infinite in  $x$  direction while being periodic in  $y$  direction. Because of this special setup, the  $p_x$  is still a good quantum number. Therefore we can do a fourier expansion in  $x$  direction:

$$c_{m,n} = \frac{1}{\sqrt{L_x}} \sum_{p_x} e^{ip_x m} c_{p_x,n} \quad (1.1.1)$$

The resulted Hamiltonian is

$$\begin{aligned} \tilde{H}_{LD} = \sum_{n,p_x} & 2 \sin(p_x) c_{p_x,n}^\dagger \sigma^x c_{p_x,n} + i \left[ c_{p_x,n+1}^\dagger \sigma^y c_{p_x,n} - c_{p_x,n+1}^\dagger \sigma^y c_{p_x,n} \right] \\ & - \left[ 2 \cos(p_x) c_{p_x,n}^\dagger \sigma^z c_{p_x,n} c_{p_x,n+1}^\dagger \sigma^z c_{p_x,n} + c_{p_x,n}^\dagger \sigma^z c_{p_x,n+1} \right] \\ & + (2 - m) c_{p_x,n}^\dagger \sigma^z c_{p_x,n} \end{aligned} \quad (1.1.2)$$

This Hamiltonian can be solved by acting it on the test wavefunction:

$$|\psi_{p_x}\rangle = \sum_n \psi_{p_x,n,u} c_{p_x,n,u}^\dagger + \psi_{p_x,n,v} c_{p_x,n,v}^\dagger |0\rangle \quad (1.1.3)$$

Note, in choosing the test wavefunction,  $u$  and  $v$  could not be separated, because there is still interaction between the two component in terms like  $c_{p_x,n}^\dagger \sigma^x c_{p_x,n}$ . If we calculate  $\tilde{H}_{LD} |\psi_{p_x}\rangle = E_{p_x} |\psi_{p_x}\rangle$ , we would get after careful calculation:

$$\begin{aligned} & \sum_n c_{p_x,n}^\dagger A \psi_{p_x,n-1} + c_{p_x,n}^\dagger B \psi_{p_x,n} + c_{p_x,n}^\dagger C \psi_{p_x,n+1} \\ & = E_{p_x} \sum_n c_{p_x,n}^\dagger \psi_{p_x,n} \end{aligned} \quad (1.1.4)$$

where

$$c_{p_x,n}^\dagger = (c_{p_x,n,u}^\dagger, c_{p_x,n,v}^\dagger) \quad (1.1.5)$$

$$A = i\sigma^y - \sigma^z \quad (1.1.6)$$

$$B = 2 \sin(p_x) \sigma^x - 2 \cos(p_x) \sigma^z + (2 - m) \sigma^z \quad (1.1.7)$$

$$C = -i\sigma^y - \sigma^z \quad (1.1.8)$$

$$\psi_{p_x,n} = \begin{pmatrix} \psi_{p_x,n,u} \\ \psi_{p_x,n,v} \end{pmatrix} \quad (1.1.9)$$

Suppose there is  $N$  lattice in the  $y$  direction. Then the periodic boundary condition implies that  $\psi_{N+1} = \psi_{n=1}$ , and  $\psi_{n=0} = \psi_N$ .

Therefore, the eigenvalue equation could be turned into a matrix form:

$$H_{\text{disc}} \psi \equiv \begin{pmatrix} B & C & & A \\ A & B & C & \\ & A & B & C \\ & & \dots & \\ & & A & B & C \\ C & & & A & B \end{pmatrix} \begin{pmatrix} \psi_{p_x,1} \\ \psi_{p_x,2} \\ \vdots \\ \psi_{p_x,N} \end{pmatrix} = E_{p_x} \begin{pmatrix} \psi_{p_x,1} \\ \psi_{p_x,2} \\ \vdots \\ \psi_{p_x,N} \end{pmatrix} \quad (1.1.10) \quad \boxed{\text{eq:disc-eigeneq}}$$

**Note:** Numerical calculations in this section are contained in the file "Lattice Dirac Model (2+1)-d.nb", and the file "Dirac\_Lattice\_Model\_21.d.m".

Let us take  $N = 3$  for simplicity. The eigenvalue problem is solved using Mathematica, and the 6 eigenvalues are:

$$\begin{pmatrix} -\sqrt{m^2 + 4m \cos(px) + 4} \\ \sqrt{m^2 + 4m \cos(px) + 4} \\ -\sqrt{m^2 + 4m \cos(px) - 6m - 12 \cos(px) + 16} \\ -\sqrt{m^2 + 4m \cos(px) - 6m - 12 \cos(px) + 16} \\ \sqrt{m^2 + 4m \cos(px) - 6m - 12 \cos(px) + 16} \\ \sqrt{m^2 + 4m \cos(px) - 6m - 12 \cos(px) + 16} \end{pmatrix} \quad (1.1.11)$$

It is found that at  $m = -2$ , there is a band crossing at  $p_x = 0$ :

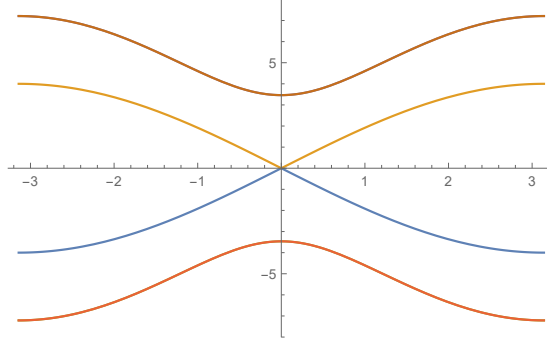


Figure 1: The Eigenvalue plot for  $m = -2$ . Plotted as  $E_{p_x}$ - $p_x$

Also, at  $m = 2$ , there is a band crossing at  $p = \pm\pi$ :

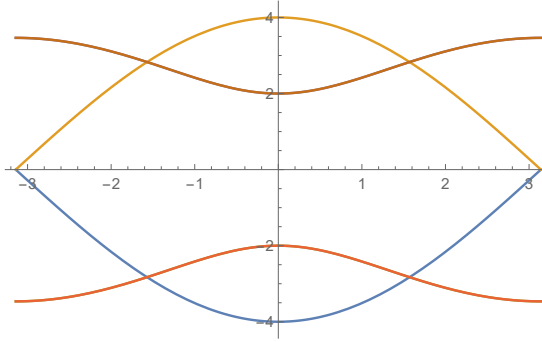


Figure 2: The Eigenvalue plot for  $m = 2$ . Plotted as  $E_{p_x}$ - $p_x$

When the band crosses, there will be two eigenvectors, corresponds to the two crossed bands, in the form of:

$$\psi_{p_x} = \left( \psi(p_x), 1, \psi(p_x), 1, \psi(p_x), 1 \right)^T \quad (1.1.12)$$

$$\phi_{p_x} = \left( \phi(p_x), 1, \phi(p_x), 1, \phi(p_x), 1 \right)^T \quad (1.1.13)$$

where  $\psi(p_x)$  and  $\phi(p_x)$  are functions of  $p_x$ . A look into the plot of  $\psi(p_x)$  and  $\phi(p_x)$  reveals that they together provide the path way for excited particles to transfer from the lower band to the upper band.

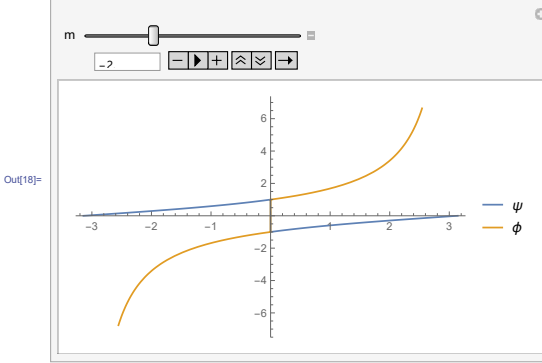


Figure 3: Plot of  $\psi(p_x)$  and  $\phi(p_x)$  when  $m = -2$

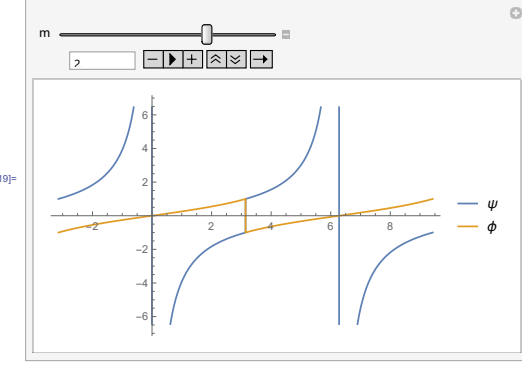


Figure 4: Plot of  $\psi(p_x)$  and  $\phi(p_x)$  when  $m = 2$ , where I have extended the plot range s.t.  $p_x \in \{-\pi, 3\pi\}$  to make the meaning clear.

Therefore, I think <sup>1</sup> this represents a pure spin-up wave transferring in the point  $p_x = 0$  when  $m = 2$ , and  $p_x = \pm\pi$  when  $m = -2$ .

### 1.1.1 Calculation Note I (Not related to the main discussion)

Since the paper will be focusing in points around  $p_x = 0$ , I focused in  $m = -2$  at first. In this case, I want to find more information about the eigenvectors.

When I looked blindly at the value  $(m, p_x) = (-2, 0)$ , the Mathematica gave me two eigenvectors both corresponds to the eigenvalue 0:

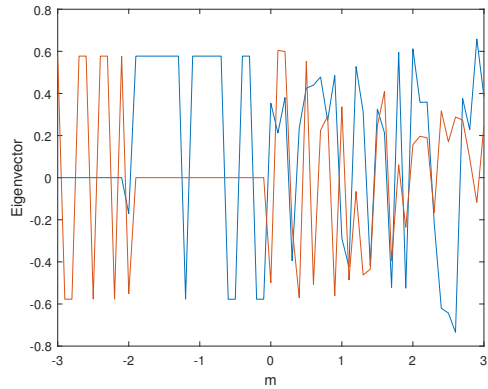
$$\{0, 1, 0, 1, 0, 1\}, \{1, 0, 1, 0, 1, 0\} \quad (1.1.14)$$

It led me to believe that there are two spin waves, with made with purely spin up waves and another of purely spin down waves. But this is not correct.

It is found later that the matrix  $H_{\text{disc}}$  is singular (with determinant 0) when  $(m, p_x) = (-2, 0)$ . Also, a Matlab calculation shows that the eigenvectors of the crossing bands actually fluctuate between  $\pm 1$  in a way illustrated as below:

---

<sup>1</sup>If I interpret the two component  $u, v$  as one for spin up and the other for spin down.



Also, the Mathematica solved eigenvector also demonstrate a drastical change around  $m = -2$ . For example, one component, when plotted against  $p_x$  change from:

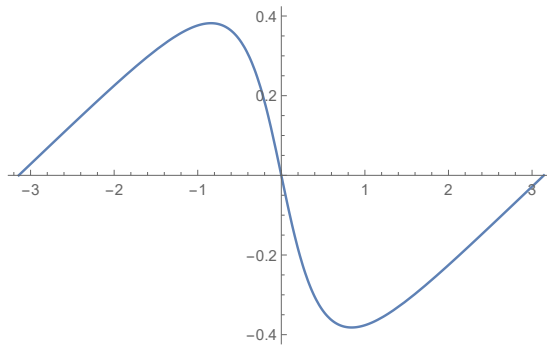


Figure 5:  $m = -3$

to

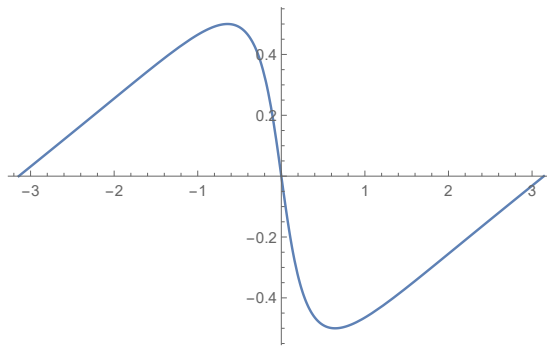


Figure 6:  $m = -2.5$

and suddenly to

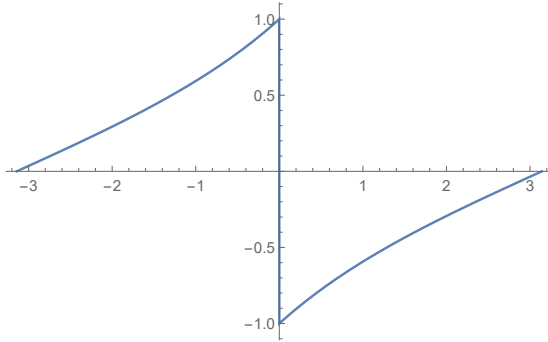


Figure 7:  $m = -2$ . There is a discontinuity at  $p_x = 0$

Finally, it becomes smooth again:

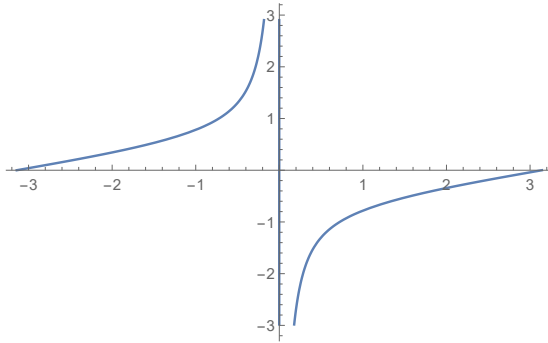


Figure 8:  $m = -1.5$

The details can be explored in the Mathematica notebook.

Also, the case of  $N = 4$  is also calculated in Mathematica. There are similarly two crossing happening at  $(m, p_x)$  equals  $(-2, 0)$  and  $(2, \pm\pi)$ .

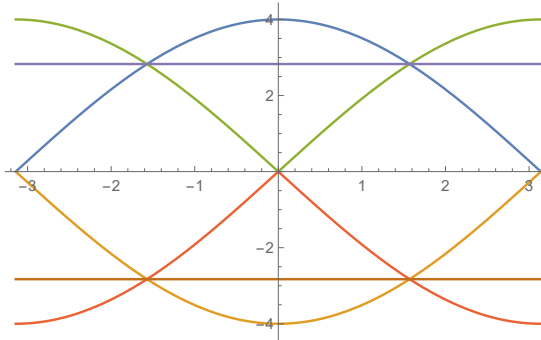


Figure 9:  $m = 2$

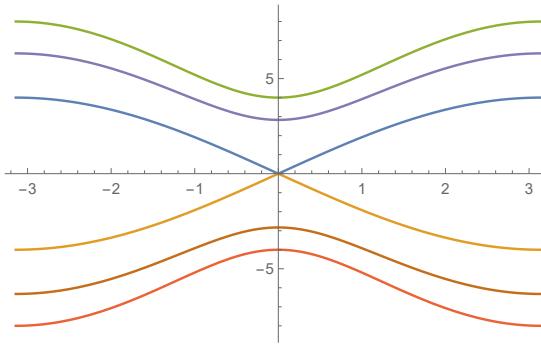


Figure 10:  $m = -2$

Surprisingly, the two bands that cross have exactly the same function dependence on  $p_x$  and  $m$  for the cases of  $N = 3$  and  $N = 4$ .

## 1.2 Why I Think the Lattice Model Hamiltonian is Mildly Wrong

I notice that equation (2.19) transformed according to (2.20) is not exactly equation (2.21), but is:

$$H = \sum_{p_x, p_y} c_{p_x, p_y}^\dagger \times [2 \sin(p_x) \sigma^x + 2 \sin(p_y) \sigma^y + (2 - m - 2 \cos(p_x) - 2 \cos(p_y)) \sigma^z] c_{p_x, p_y} \quad (1.2.1)$$

This result does not become the continuum Dirac Hamiltonian as  $p_x, p_y$  goes to zero. Therefore, I suspect that certain constants should be modified so that:

$$H_{LD} = \sum_{m,n} \left\{ \frac{i}{2} \left[ c_{m+1,n}^\dagger \sigma^x c_{m,n} - c_{m,n}^\dagger \sigma^x c_{m+1,n} \right] + \frac{i}{2} \left[ c_{m,n+1}^\dagger \sigma^y c_{m,n} - c_{m,n}^\dagger \sigma^y c_{m,n+1} \right] \right. \\ \left. - \frac{1}{2} \left[ c_{m+1,n}^\dagger \sigma^z c_{m,n} + c_{m,n}^\dagger \sigma^z c_{m+1,n} + c_{m,n+1}^\dagger \sigma^z c_{m,n} + c_{m,n}^\dagger \sigma^z c_{m,n+1} \right] \right. \\ \left. + (2-m)c_{m,n}^\dagger \sigma^z c_{m,n} \right\} \quad (1.2.2)$$

This affects the numerical analysis effectively by the replacement

$$\sigma^i \rightarrow \frac{1}{2}\sigma^i, \quad (2-m) \rightarrow 2(2-m)$$

The calculated result is similar to that in the previous section, except that the band crossing happens at different values of  $m$ . <sup>2</sup> So the essential point is unaltered by the difference in some constants. However, in the correct calculation, the crossing band appears at  $m = 0$ , which represents a massless spin- $\frac{1}{2}$  particle. I think this should have some theoretical implications.

### 1.3 Solution With Translational Invariance (Bloch States) in both x and y (Infinite Plane)

#### 1.3.1 Numerical Solution

**Note 1:** Since the essential point is not altered by the minor error in Hamiltonian, as mentioned in Section 1.2. I will continue with the Lattice Model Hamiltonian that produce correctly the Dirac Hamiltonian in the continuum limit.

**Note 2:** Calculation in this part is available in the Mathematica notebook "Lattice Dirac Model (2+1)-d-2.nb".

When the two sides are of open boundary, the problem is quite simple and the Fourier-transformed Hamiltonian is (almost) diagonal in momentum space. It is (as calculated in [Hug09], eq.2.21):

$$H = \sum_{p_x,p_y} c_{p_x,p_y}^\dagger \times \\ [\sin(p_x)\sigma^x + \sin(p_y)\sigma^y + (2 - m - \cos(p_x) - \cos(p_y))\sigma^z] c_{p_x,p_y} \quad (1.3.1)$$

The eigenvalues of the Hamiltonian of the form  $\mathbf{a} \cdot \boldsymbol{\sigma}$  are:

$$E_1 = |a|, \quad E_2 = -|a| \quad (1.3.2)$$

If plotted in  $(p_x, p_y)$  plane, we will find several interesting crossing happening when  $m = 0, 2, 4$ :

---

<sup>2</sup>For example, the eigenvalue of original and the modified equation (2.21) are plotted in Mathematica notebook "Eq2.21-Demo.nb". Also, the solution to the infinite cylinder boundary condition has again two band crossings, each at  $(m, p_x)$  equals  $(0, 0)$  and  $(2, \pm\pi)$  (for  $N = 3$  case).

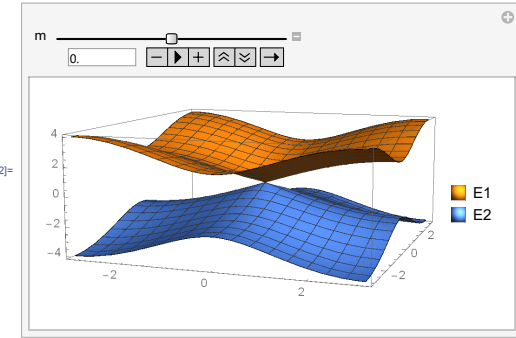


Figure 11:  $m = 0$

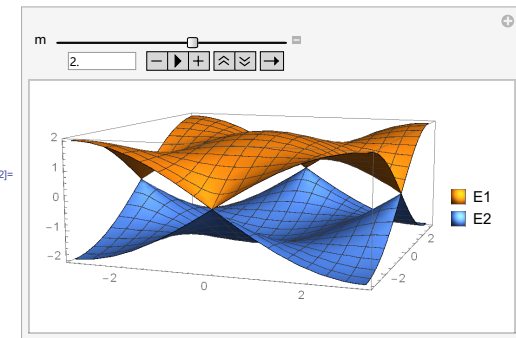


Figure 12:  $m = 2$

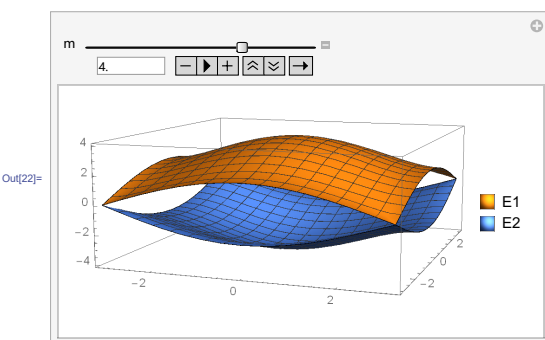


Figure 13:  $m = 4$

The eigenvectors are of the form:

$$(\phi, \sin(p_x) + i \cos(p_y)), \quad (\psi, \sin(p_x) + i \cos(p_y)) \quad (1.3.3)$$

where

$$\phi = (2 - m - \cos(p_x) - \cos(p_y)) + E_1 \quad (1.3.4)$$

$$\psi = (2 - m - \cos(p_x) + \cos(p_y)) + E_1 \quad (1.3.5)$$

And besides crossing each other, they have new interesting behavior as  $m$  varies. When changing from  $m = -1$  to  $m = 6$ , they gradually contact and exchange the position of each other <sup>3</sup>:

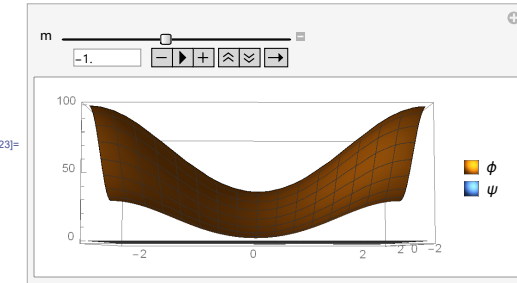


Figure 14:  $m = -1$

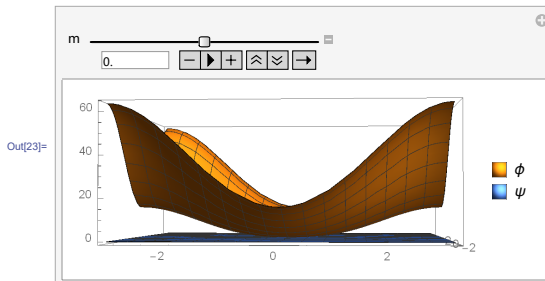


Figure 15:  $m = 0$

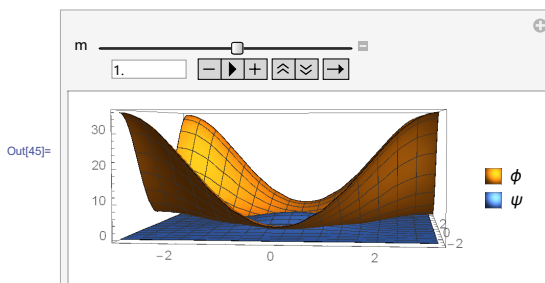


Figure 16:  $m = 1$

---

<sup>3</sup>You would get more fun if you execute the animation inside the Mathematica notebook

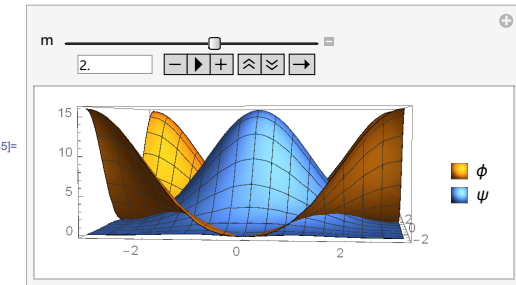


Figure 17:  $m = 2$

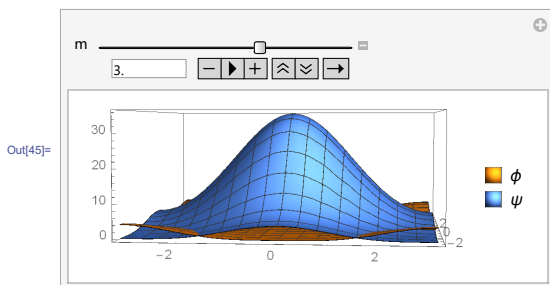


Figure 18:  $m = 3$

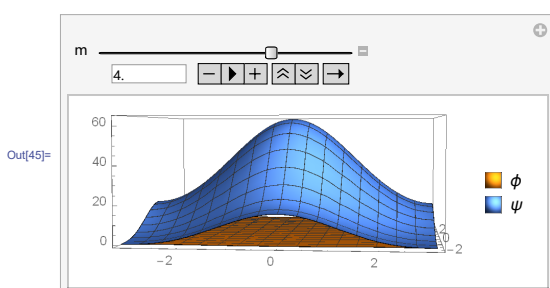


Figure 19:  $m = 4$

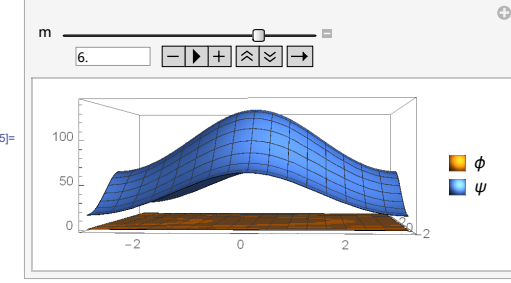


Figure 20:  $m = 6$

## 1.4 Solution With Translational Invariance in x, and Open Boundary in y (Infinite Stripe)

Calculations in this are contained in files:

- [Lattice Dirac Model \(2+1\)-d-4-Infinite Stripe \(N=3\).nb](#),
- [Lattice Dirac Model \(2+1\)-d-4-Infinite Stripe \(N=20\).nb](#),
- [Lattice Dirac Model \(2+1\)-d-4-Infinite Stripe \(N=30\).nb](#),

This amounts to removing the  $A$  in top right corner and  $C$  in bottom left corner of eq.1.1.10. In this case, the crossing bands exists at slightly different value of  $m$ , also, there are few sharp transitions from a closed gap state, to an open gap state. For example, when  $N = 3$ , the band crossing happens at two ranges of  $m$ : from 0 to 2 and from 2 to 4 (shown in Figure 21). The cases when  $N = 10$ ,  $N = 20$ ,  $N = 30$  also exhibits similar behavior. They also have almost two ranges of values for  $m$  when two bands close at one point. Their result are plotted are at fig 22, fig 23, and fig 24.

As we have seen, the solution by Mathematica is analytically intractable as  $N$  grows larger. Also it would be too time-consuming if I were to plotting those eigenvectors when  $N$  is large. So I looked for similar things inside the book by Bernevig [BH13], and found the following model.

### 1.4.1 Edge States in Continuum Limit

I will analyse the continuum limit of this model at the point  $(p_x = 0, p_y = 0)$ , where the energy  $E = 0$ . I also assume that we have placed to materials adjacent to each other in  $x$  direction. I will assume that the two materials are in different topological states. For example, if the band cross when  $m = 0$ , then one material will have  $m < 1$ , and the other will have  $m > 0$ . Therefore, at the interface, we could have  $m$  as a function of  $x$  such that  $m(0) = 0$ .

This assumption implies that we break translational in both direction. So at this point  $p_x = 0$ ,  $\sin(p_x) \rightarrow p_x$ , and is replaced by  $-i\hbar\partial_x$ . Similar for  $\sin(p_y)$ . So we recovered the continuum model:

$$H = -i\hbar\partial_x\sigma^x - i\hbar\partial_y\sigma^y - m\sigma^z \quad (1.4.1)$$

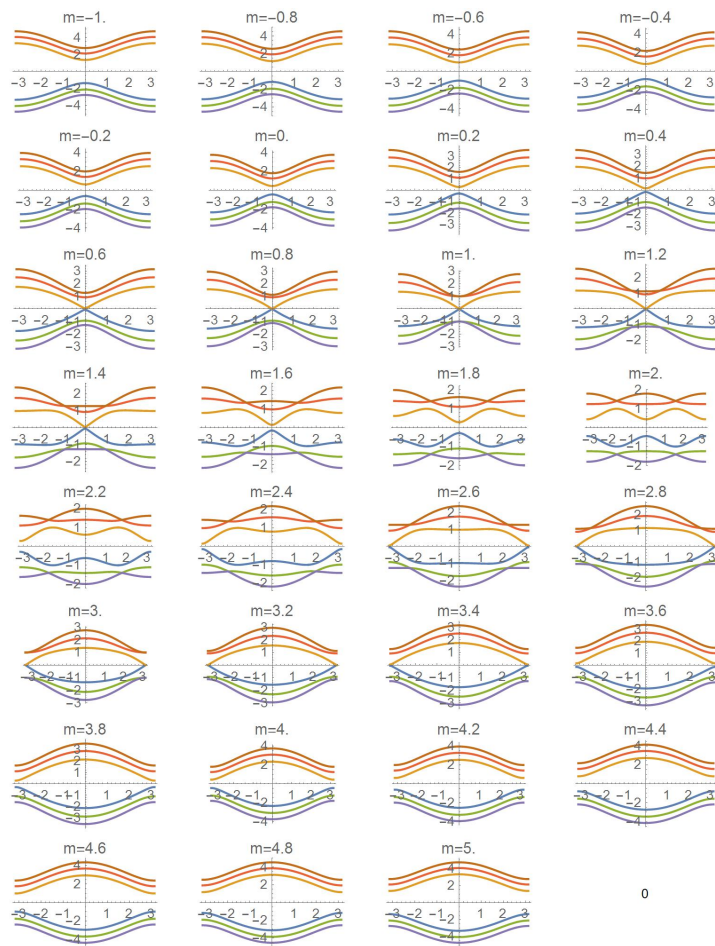


Figure 21: Infinite Strip,  $N = 3$

`fig:InfiniteStrip=3.jpg`

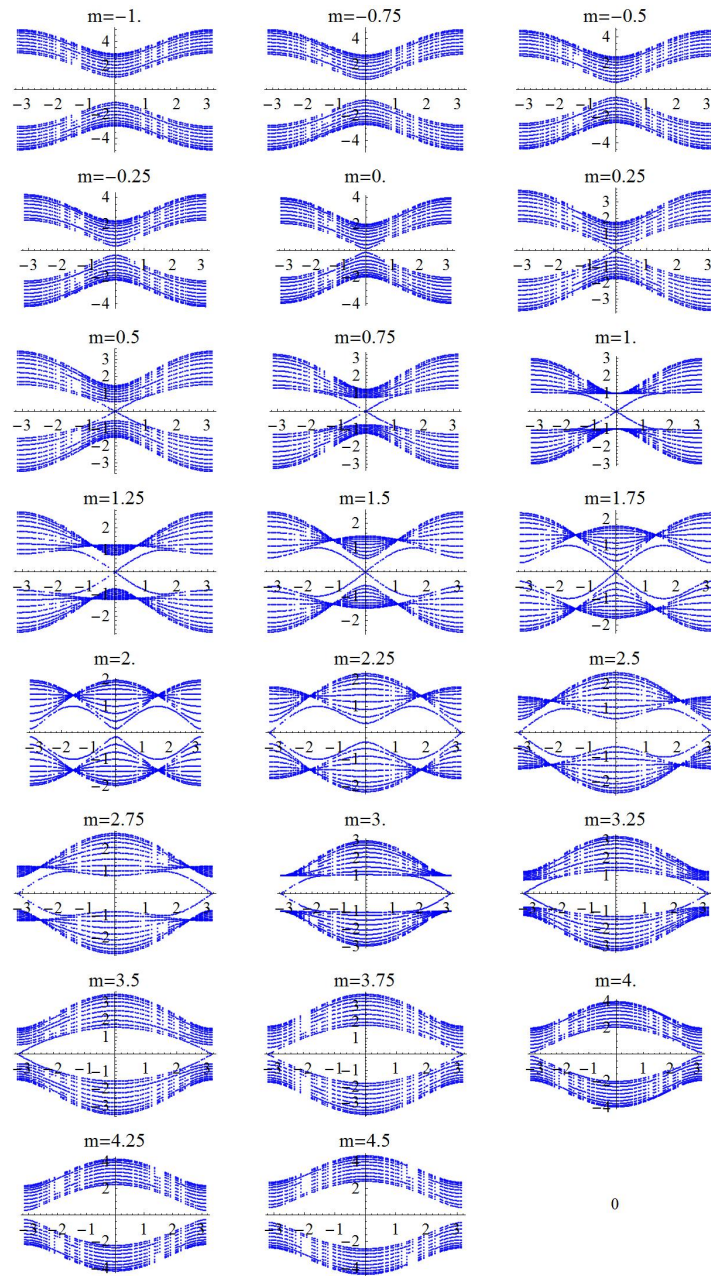


Figure 22: Infinite Strip,  $N = 10$

`fig:InfiniteStrip=10.jpg`

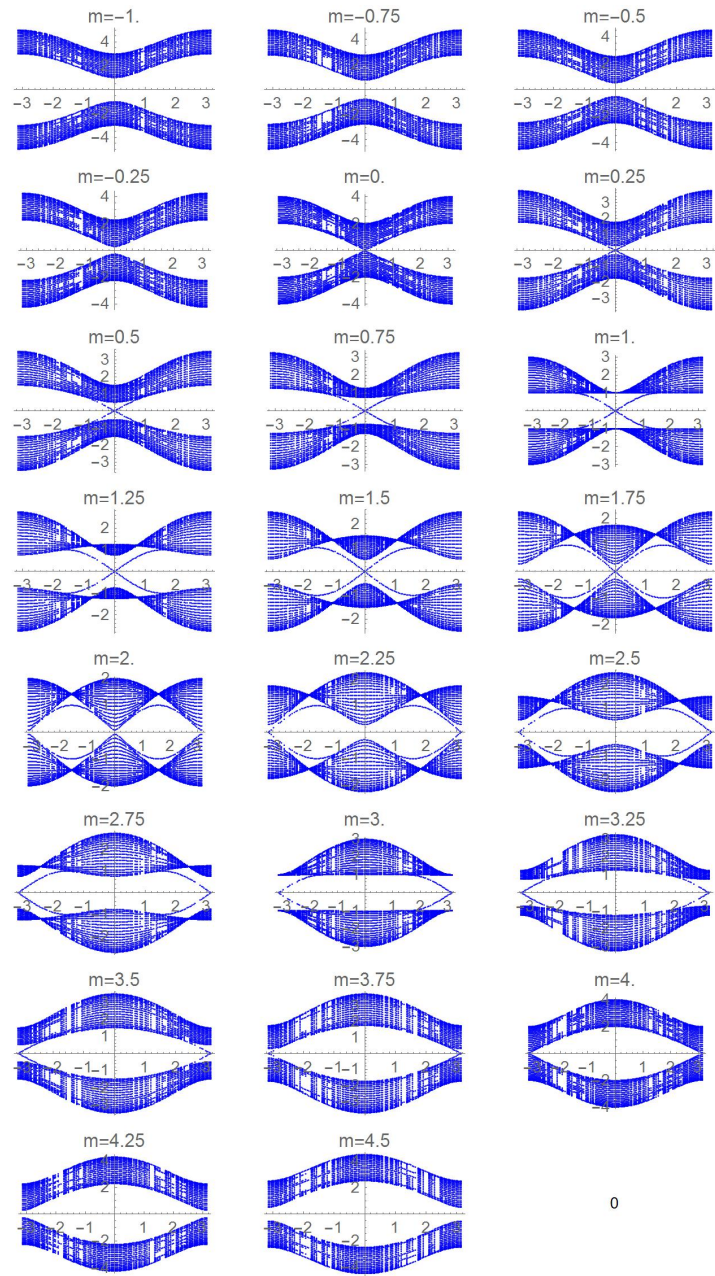


Figure 23: Infinite Strip,  $N = 20$

fig:InfiniteStrip=20.jpg

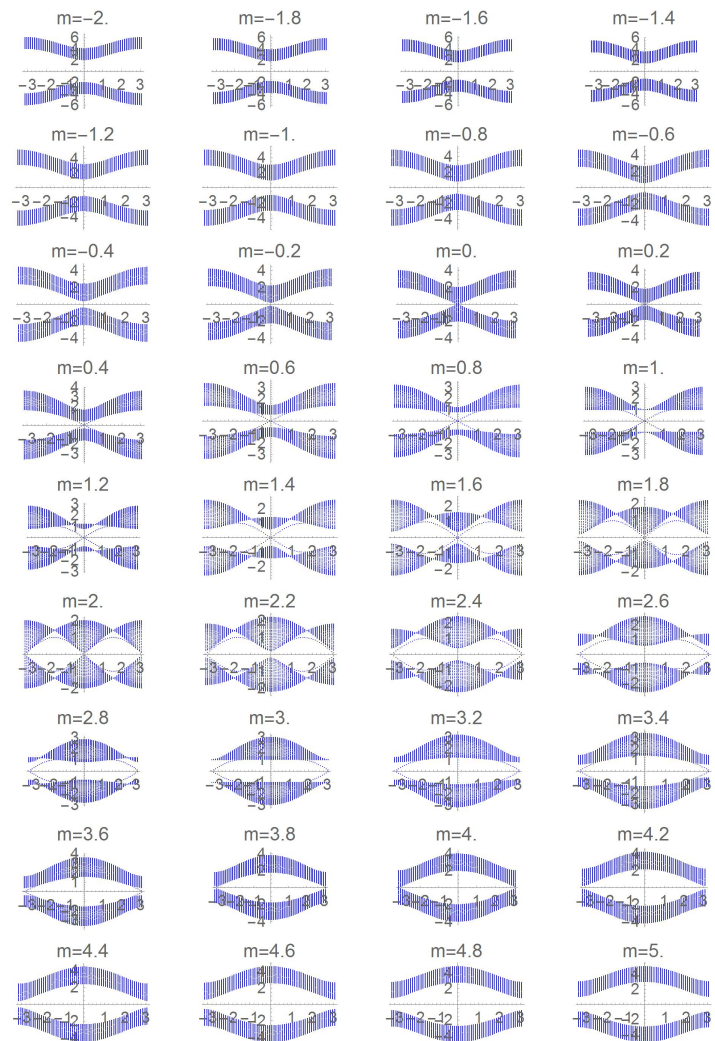


Figure 24: Infinite Strip,  $N = 30$

`fig:InfiniteStrip=30.jpg`

The Schrodinger equation is  $H\psi = E\psi = 0$  for  $E \approx 0$  around this point. After some calculations, the equation is (with  $\hbar = 1$ ):

$$[i\partial_x\sigma^x + i\partial_y\sigma^y + m\sigma^z]\psi = 0 \quad (1.4.2)$$

However, this coupled PDE is hard to solve by Mathematica<sup>4</sup>. Therefore, I restrict their value on  $x$ , and solve the ODE:

$$i\partial_x\psi_2(x) + m\psi_1(x) = 0 \quad (1.4.3)$$

$$i\partial_x\psi_1(x) - m\psi_2(x) = 0 \quad (1.4.4)$$

If assuming  $m(x)$  is in the form of  $m(x) = x$ , i.e. positive when  $x > 0$ , and negative when  $x < 0$ , then the solution is:

$$\psi_1(x, y) = e^{\text{Int}(x)}C(y) \quad (1.4.5)$$

$$\psi_2(x, y) = -i\psi_1(x, y) \quad (1.4.6)$$

where  $\text{Int}(x) = \int_1^x -m(k) dk$ .  $\text{Int}(x)$  has the property of goes to  $-\infty$  as  $x \rightarrow \pm\infty$ .

If, on the contrary, assuming  $m(x)$  is in the form of  $m(x) = -x$ , i.e. positive when  $x < 0$ , and negative when  $x > 0$ , then the solution is:

$$\psi_1(x, y) = e^{-\text{Int}(x)}C(y) \quad (1.4.7)$$

$$\psi_2(x, y) = i\psi_1(x, y) \quad (1.4.8)$$

In both cases, the function are exponentially decaying wave in the interface at  $m(0) = 0$ .

Paused to think what I have got. I have in essential got a solution separated in  $x, y$ . Therefore, now I re-solve this edge mode, using technique of separation of variables<sup>5</sup>.

Without loss of generality, assume  $m(x)$  is like  $x$ , i.e. it goes to  $\pm\infty$  as  $x \rightarrow \pm\infty$ . Then, separate the wavefunction into:

$$\psi(x, y) = \phi_1(x)\phi_2(y) \quad (1.4.9)$$

Assuming we are solving a Schrodinger equation  $H\psi = E\psi$ , with  $E$  being very small. Now, inspired by previous calculation, write down directly  $\phi_1(x) = e^{-\int_0^x m(x') dx'}$ . Then, the equation decoupled directly into:

$$(-i\sigma_y\partial_y + m(x)(i\sigma_x - \sigma_z))\psi_2(y) = E\psi_2(y) \quad (1.4.10)$$

Since  $E$  is small, but  $m(x)$  could be very large and is independent of  $y$ , we should make the term  $(i\sigma_x - \sigma_z)$  somehow disappear. This matrix is singular and has only eigenvalue 0. Its eigenvector is  $(i, 1)^t$ . So we assume  $\phi_2(y) = \chi(y)(i, 1)^t$ .

It turns out that  $(i, 1)^t$  is also the eigenvector of  $\sigma_y$  with eigenvalue  $-1$ . So the equation becomes quite simple now:

$$i\partial_y\chi(y) = E\chi(y) \quad (1.4.11)$$

The solution is  $\chi(y) = e^{-iEy}$ , a free electron in the  $y$  direction!

---

<sup>4</sup>See file `Lattice Dirac Model (2+1)-d-3-EdgeStates.nb` for my calculations.

<sup>5</sup>Actually, I am just mimicking the calculation in section 8.8 of [BH13].

**Remark 1.1.** Although the above calculation breaks translational invariance in both direction, the actual boundary states breaks only one. Nonetheless, I could do almost the same calculation with  $p_y$  conserved, e.g. in a infinite strip. In that case, I would get a state localized in the interface, and have  $p_y = -E$ , representing an electron travelling with momentum  $-E$  in  $y$ 's direction.

### 1.4.2 Edge State in Infinity Strip

The edge state in this infinite strip (translational invariant in  $x$ , and open boundary in  $y$ ) is difficult is obtain. The eigenvalue equation 1.1.10 gives the following relation:

$$A\psi_{n-1} + B\psi_n + C\psi_{n+1} = E\psi_n \quad (1.4.12)$$

If  $A, B, C$  are numbers (or invertible matrices), then we could express  $\psi_1$  in turns of  $\psi_N$  (assuming  $E = 0$ ) and take the limit  $\psi_1/\psi_N = 0$  or  $\infty$ . This would hint a boundary state localized in 1 or  $N$ .

But now  $A$  and  $C$  are singular, this makes the equation 1.4.12 mostly undetermined. The simplest case is that when  $B = 0$  (i.e. when  $p_x = 0$  or  $\pm\pi$ , and  $2 - m - \cos(p_x) = 0$ , thus  $m = 1$  or  $3$ ), there are four possible eigenstates of eigenvalue  $E = 0$ :

$$\begin{aligned} \psi_N &= \begin{pmatrix} 1 \\ -1 \end{pmatrix} \text{ or } \begin{pmatrix} 0 \\ 0 \end{pmatrix}, \quad \psi_1 = \begin{pmatrix} 1 \\ 1 \end{pmatrix} \text{ or } \begin{pmatrix} 0 \\ 0 \end{pmatrix} \\ \psi_{N-1} &= \psi_{N-2} = \dots = \psi_2 = \begin{pmatrix} 0 \\ 0 \end{pmatrix} \end{aligned} \quad (1.4.13)$$

This shows that it possibly has states localized at the boundary, but this tells us nothing when  $m$  is not the prescribed values(1 and 3).

## 1.5 Berry Phase

sec:Berry Phase

The easiest case when we can calculate the Berry phase is when we have translational invariance in both  $x$  and  $y$  direction. The Fourier-transformed Hamiltonian is then diagonal.

$$H = \sum_{p_x, p_y} c_{p_x, p_y}^\dagger \times [\sin(p_x)\sigma^x + \sin(p_y)\sigma^y + (2 - m - \cos(p_x) - \cos(p_y))\sigma^z] c_{p_x, p_y} \quad (1.5.1)$$

The Berry phase for a Hamiltonian of the form  $\vec{d}(\vec{k}) \cdot \vec{\sigma}$ , is equal to  $\pm\frac{1}{2}\Omega$ , where the sign is determined by the choice of eigenstate, the  $\Omega$  is the solid angle traversed by  $\vec{d}$  as its parameter  $\vec{k}$  varies, Now  $\vec{d} = (\sin(p_x), \sin(p_y), 2 - m - \cos(p_x) - \cos(p_y))$ , which is numerical explored<sup>6</sup>.

The surface of  $\vec{d}$  as  $p_x, p_y$  varies is somewhat distorted (fig 25). Thankfully, it does not change as  $m$  varies (fig 26). Also, it is easy to see that when  $m < 0$  or  $m > 4$ , the surface does not cut the  $xy$  plane, hence in that region the Berry Phase is trivial. The distorted picture is dispatched into

<sup>6</sup>Details can be found in in file [Attempts at Getting Chern Number.nb](#).

4 different pieces in fig 27. It could be imagined that the vector  $\vec{d}$  goes in the order: red → blue → yellow → green → red. With this and a little bit of imagination, I think the solid angle  $\Omega$  when  $0 < m < 2$  and  $2 < m < 4$  are both  $4\pi$ .

Exact value can be found using the formula for solid angle in a parameterized surface. Assuming the surface is parameterized as

$$\vec{f}(x, y) = (f_1(x, y), f_2(x, y), f_3(x, y)) \quad (1.5.2)$$

Its solid angle can be calculated by:

$$\int dx dy \frac{\vec{f}(x, y)}{|\vec{f}(x, y)|^3} \partial_x \vec{f}(x, y) \times \partial_y \vec{f}(x, y) \quad (1.5.3)$$

This formula can be understood mathematically [Mat], and calculated physically (see p.216 of [She12]). The calculated result for different  $m$  is plotted in fig 28.

$m=1$

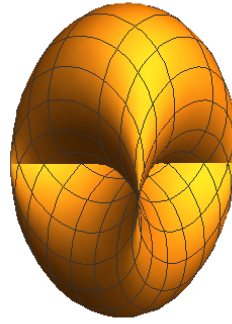


Figure 25: Surface formed as  $p_x, p_y$  varies

`fig:BerryPhase/Shape`

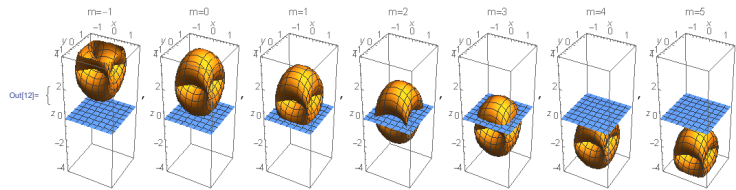


Figure 26: As  $m$  varies, the shape does not change. The blue plane is the  $xy$ -plane. The center of that surface meets the  $xy$ -plane when  $m = 2$ . That surface leaves the  $xy$ -plane when  $m < 0$  or  $m > 4$ .

`fig:BerryPhase/AsMVaries`

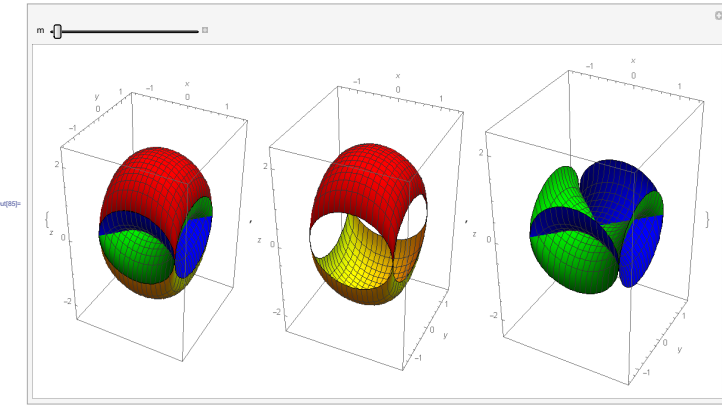


Figure 27: Attempts to determine the Berry phase by dispatching the surface into 4 different patches ( $m = 2$ )

`fig:BerryPhase/attempts`

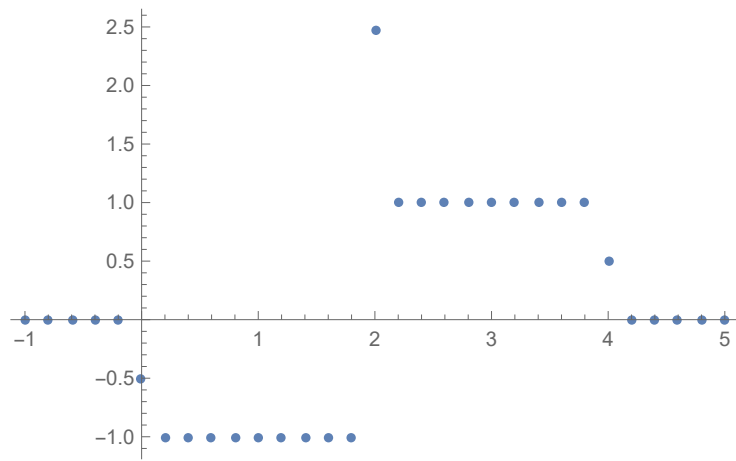


Figure 28: Plot of Chern Number for different  $m$ .

`fig:BerryPhase/SSQFormula`

## 2 License

The entire content of this work (including the source code for TeX files and the generated PDF documents) by Hongxiang Chen (nicknamed we.taper, or just Taper) is licensed under a Creative Commons Attribution-NonCommercial-ShareAlike 4.0 International License. Permissions beyond the scope of this license may be available at [mailto:we.taper\[at\]gmail\[dot\]com](mailto:we.taper[at]gmail[dot]com).

## References

- [BH13] B A Bernevig and T L Hughes. *Topological Insulators and Topological Superconductors*. Princeton University Press, 2013. URL: [https://books.google.co.jp/books?id={\\_}7r{\\_}UqFNOIEhttp://press.princeton.edu/titles/10039.html](https://books.google.co.jp/books?id={_}7r{_}UqFNOIEhttp://press.princeton.edu/titles/10039.html).
- [Hug09] Taylor Hughes. *Time-reversal Invariant Topological Insulators*. PhD thesis, Stanford University, 2009. URL: <http://gradworks.umi.com/33/82/3382746.html>.
- [Mat] MathOverflow. How do you calculate the solid angle of a rectangular, axis aligned section of a surface defined by a two dimensional function? URL: <https://mathoverflow.net/q/63231>.
- [She12] Shun-Qing Shen. *Topological Insulators*, volume 174 of *Springer Series in Solid-State Sciences*. Springer Berlin Heidelberg, Berlin, Heidelberg, 2012. URL: <http://link.springer.com/10.1007/978-3-642-32858-9>, doi:10.1007/978-3-642-32858-9.